Advanced Powder Technology 30 (2019) 961–973

Contents lists available at ScienceDirect

Advanced Powder Technology

journal homepage: www.elsevier.com/locate/apt

Original Research Paper

Functionality improvement of Nimesulide by eutectic formation with nicotinamide: Exploration using temperature-composition phase diagram

Rajeshri D. Patel [a], Mihir K. Raval [a,*], Ajrudeen A. Bagathariya [a], Navin R. Sheth [b]

[a] Department of Pharmaceutical Sciences, Saurashtra University, Rajkot 360 005, Gujarat, India
[b] Gujarat Technological University, Ahmedabad 382 424, Gujarat, India

ARTICLE INFO

Article history:
Received 10 May 2018
Received in revised form 11 February 2019
Accepted 13 February 2019
Available online 22 February 2019

Keywords:
Nimesulide
Nicotinamide
Eutectic
Thermal-composition phase diagram
Physico-mechanical property

ABSTRACT

The aim of present work was to explore the temperature-composition phase diagram for detection of formation of a multi-component system. Fusion of model drug Nimesulide (NIM) and Nicotinamide (NIC) was prepared and evaluated for possible interaction using thermal analysis. Phase diagram and the appearance of single endotherm confirmed Eutectic formation with the molar ratio of 1:2 (NIM: NIC). Spray dried powder in same molar ratio showed improved functionality in terms of solubility (14 folds), dissolution (2 folds) in distilled water and drug content (92.27%). SEM study revealed that the particles of eutectic mixture were of nearly same size in all directions in shape with bigger particle size compared to the pure drug, which was responsible for its improved flow. The compressibility of prepared eutectic was greatly enhanced which was followed by formation of directly compressible tablets. FT-IR study explained the possibility of formation of hydrogen bond between both the components. Stability data proved the stable nature of the eutectic mixture as well as its prepared formulation. The study explained the way to prepare thermal phase diagram by taking solidus and liquidus points in DSC diagram, which was finally used as a confirmatory parameter for the formation of the eutectic. Simultaneous improvement in physicochemical and mechanical properties was highlighted.

1. Introduction

As far as the research and development in pharmaceutical industries is concerned, poor solubility and dissolution of APIs are one of the biggest problems. Majority of already existing molecules and new molecules under the drug discovery process are poorly water-soluble [1]. Pharmaceutical industries are facing a big challenge to convert such molecules into a robust formulation within the preview of regulatory constraints.

Various methods like solid dispersion [2], SEDDS [3], milling [4], complexation [5], co-solvency [6], polymorphic modifications [7], nanotechnology [8] and many more have been tried to improve the physicochemical properties of APIs like solubility and dissolution.

There are many more APIs which are poor not only in physicochemical properties but also in flow properties and compressibility. Such API requires a large quantity of glidants and binders in their manufacturing. It again cost a lot to the industries and industry has no choice except to go for multi-step, more laborious, costly wet granulation process instead of much cheaper and time-labour saving direct compression process [9,10].

It is very important to understand that for any robust formulation, not only the physicochemical properties but also the mechanical properties should be satisfactory. Very few research works are going on such processes which can improve the functionality of API in all dimensions. Means, a common technique which can improve physic-mechanical properties of APIs have great importance in industrial research.

Various techniques have been followed to manipulate the functionality of APIs and to address the problems raised in the formulation. Salt and hydrates formation is widely utilized to improve the solubility and dissolution of APIs. As far as neutral or weakly acidic drugs are concerned, it is very difficult to prepare salt due

Abbreviations: NIM, Nimesulide; NIC, nicotinamide; DSC, differential scanning calorimetry; PXRD, powder X-ray diffraction; FT-IR, Fourier transform infrared spectroscopy; SEM, scanning electron microscopy.

* Corresponding author.
E-mail address: mkraval@sauuni.ernet.in (M.K. Raval).

https://doi.org/10.1016/j.apt.2019.02.010
0921-8831/

to poor proton transfer capacity [11]. In such cases, cocrystallization can play a crucial role in the overall improvement of the functionality of APIs. In this process, API and coformer material are interacting with each other in a particular molar ratio by a certain kind of supramolecular complex formation [12]. In majority cases, eutectic, solid solution or cocrystal formation is resulted mainly due to the interaction happens between supramolecular synthones. There are various examples available which suggest that if the homomolecular (cohesive) interactions predominate with the isomorphous materials, solid solutions are formed whereas, with the non- isomorphous materials, eutectics are produced. Conversely, if the heteromolecular (adhesive) interactions between targeted molecules, it results in cocrystal formation [13–15].

After X-ray diffraction technique, thermal technique specifically Differential scanning calorimetry (DSC) is most approachable and accurate to determine the formation of cocrystal or eutectic. Various research works have been published where the thermal method has been used to determine the formation of any of these forms, but still, it is difficult to understand for beginners to interpret thermal events. As per literature, thermal behaviours by DSC diagrams (at the low heating rate) give a single endothermic peak in case of eutectic formation whereas in case of cocrystal. As explained in Fig. 1, the individual component A and B melt together followed by formation of a cocrystal at the metastable eutectic point. This event can be described by an endotherm immediately followed by an exothermic peak. On further heating, the cocrystal of A and B (AB) melts which is illustrated by a second endothermic peak (Fig. 1A and A-1). At the same time, if the solid A and B do not have the capability to form cocrystal, a single sharp endothermic peak in DSC shows eutectic melting of A and B (Fig. 1B and B-1) [16].

Vasisht et al. generated highly soluble eutectics with improved biological efficacy of hesperetin which was decided by the thermal phase diagram [17]. Dalvi and Sathisaran constructed a binary phase diagram for the curcumin-salicylic acid system which resulted in the formation of eutectic at curcumin mole fraction of 0.33 [18]. Bansal et al. investigated that microstructure of aspirin-paracetamol eutectic system offered greater compressibility, tabletability, and compactibility as compared with the physical mixture of that system [19]. Sangamwar et al. studied the eutectic mixture of α-eprosartan with p-hydroxybenzoic acid in 1:3 stoichiometry ratio showed better physicochemical and pharmacokinetic behaviour compared to parent drug [20]. Various other APIs and their eutectics like etodolac with paracetamol and propranolol hydrochloride [21], simvastatin-aspirin [22], hydrochlorothiazide-atenolol [23] and felodipine-nicotinamide [24] have been reported for their improved properties.

Here, authors have tried to explore the thermal technique for determination of formation of new solid material and its molar ratio by using Nimesulide (NIM) as a model drug and Nicotinamide (NIC) as coformer.

Nimesulide chemically 4′-Nitro-2′-phenoxy methane sulfonanilide, is a weakly acidic nonsteroidal anti-inflammatory drug (Fig. 2). Nimesulide is considered a BCS class II drug and is very sparingly soluble in water (≈0.01 mg/ml). Moreover, Nimesulide have poor flowability character. Due to poor aqueous solubility and wettability, Nimesulide leads to difficulties in pharmaceutical formulations for oral or parenteral delivery.

The selection of coformer can be determined by understanding supramolecular synthon, pKa difference, molecular weight, Hansen solubility parameter and melting point [25]. Here, Nicotinamide (NIC), 3-Pyridinecarboxamide, was used as hydrophilic conformer (aqueous solubility is 500 g/L) in the context of non-covalent derivative forms [26]. NIC contains nitrogen atom at the pyridine group and amide group can easily form homosynthon or heterosynthon with NIM [27]. Authors have used DSC as a thermal technique to prepare fusion of drug and coformer to determine the formation of crystal form followed by spray drying to generate a

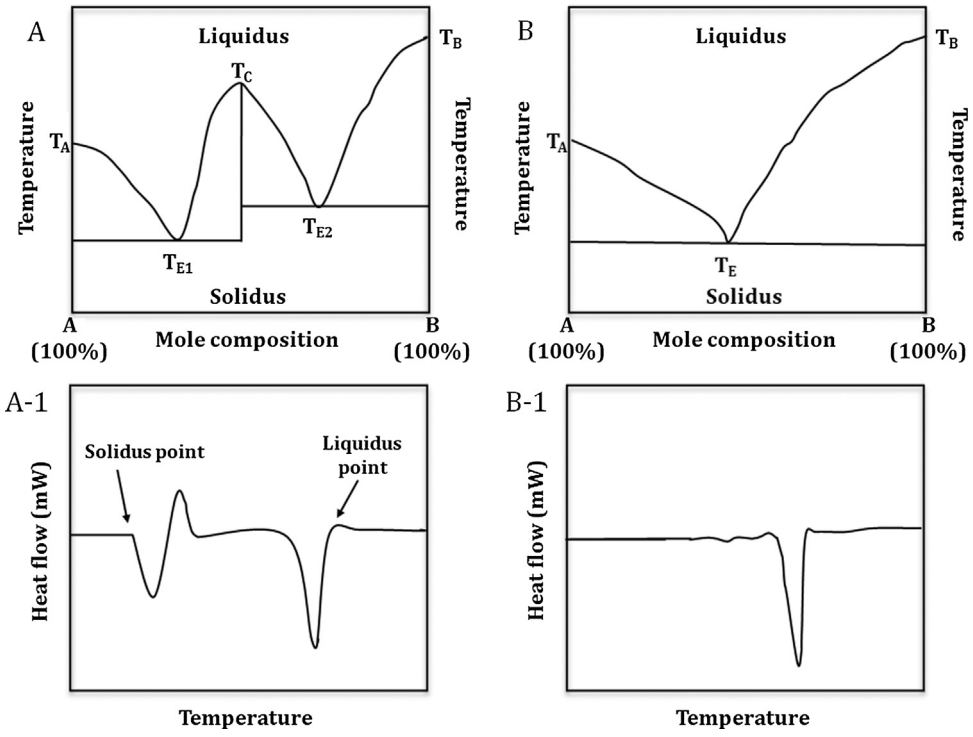

Fig. 1. Schematic illustration of binary phase diagram and DSC thermogram of cocrystal formation (A, A-1) and eutectic formation (B, B-1) respectively. T_A, melting temperature of compound A; T_B, melting temperature of compound B; T_C, melting temperature of cocrystal; T_E, eutectic melting temperature; T_{E1}, eutectic temperature 1; T_{E2}, eutectic temperature 2.

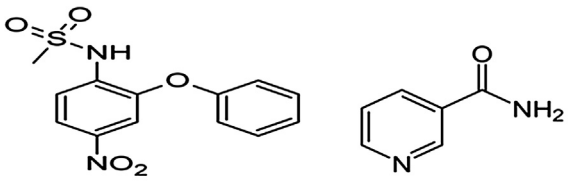

Fig. 2. Chemical structure of Nimesulide and Nicotinamide used in this study.

cocrystallized material having improved solubility, dissolution and other mechanical properties. Finally, the material was converted into a directly compressible formulation as a tablet dosage form.

2. Materials and methods

2.1. Materials

Nimesulide (NIM) and Nicotinamide (NIC) were procured from Nectar Drug Pvt. Ltd. (Mumbai, India) and Sisco Research Laboratories Pvt. Ltd., (Mumbai, India), respectively. All other chemicals and solvents used were of analytical grade. Distilled water was generated from a Millipore Direct—Q ultra-pure water system (Merck Millipore, India).

2.2. Thermal-composition phase diagram for the screening study

NIM (308.3 g/mol) and NIC (122.1 g/mol) in various molar ratios (NIM:NIC) like 10:0, 9:1, 8:2, 7:3, 6:4, 5:5, 4:6, 3:7, 2:8, 1:9 and 0:10 mixed together in porcelain china plate to maintain the total quantity of 500 mg in every ratio. Mixtures were heated on heating plate corresponding to a temperature 2 °C above that of the melting temperature of the substance having the highest melting temperature. This completely fused liquid was poured in glass Petri plate, previously heated in order to avoid the sudden quenching of heat. After stirring for a few seconds, the melted mixture was allowed to cool and solidified rapidly on an ice bath with vigorous stirring. The final solid mass was stored in glass vial inside desiccator. Phase diagram was constructed by taking solidus and liquidus values obtained from a thermal analysis of various cocrystallized mixtures of said combinations in various mole fractions [28].

2.3. Preparation of multi-component solid form using spray drying technique

Various techniques were tried for scaling up (Data not shown here) and spray drying was selected finally for preparation of large batch [29]. Spray dried solid forms were prepared using laboratory spray dryer (LU 222 ADVANCED, Labultima, Mumbai, India). NIM and NIC were dissolved in methanol (each batch size was maintained at approx. 20gm). Prepared organic solutions were spray dried at an optimum condition by taking feed rate- 2 ml/min, inlet drying air temperature 90–100 °C, aspirator air flow 50–60 Nm^2/h and the outlet temperatures in the range of 40–50 °C. The spray-dried powders were recovered from cyclone collector and stored in a desiccator at ambient temperature for 24 h.

2.4. Solid state characterization study

2.4.1. Differential scanning calorimetry (DSC) study

DSC analysis of the cocrystallized samples was performed on a DSC 60 (Shimadzu, Tokyo, Japan) previously calibrated for temperature and heat flow accurately using indium. Accurately weighed samples (3 mg) were placed in hermetically sealed aluminium pans and heated through the corresponding melting temperature range at a scan speed of 5 °C/min using nitrogen purging at 100 ml/min. Endotherms were recorded from 40 to 300 °C against a sealed aluminium empty crucible as a reference.

2.4.2. Fourier transmission Infra-Red spectroscopy (FTIR)

FTIR spectra were obtained using Infrared spectrophotometer (Nicolet IS 10, Thermoscientific, Japan). The samples were dispersed in KBr and compressed into disc/pellet by application of pressure (KBr press). The pellets were placed in the light path for recording the IR spectra. The spectrum was recorded in the region of 400–4000 cm^{-1}.

2.4.3. Powder X-Ray diffraction analysis (PXRD)

The PXRD patterns of pure drug and optimized samples were recorded using PANalytical diffractometer system (Xpert pro-Multi-Purpose Diffractometer, Philips, Mumbai, India) with a radiation and scintillation counter detector (voltage 40 kV; current 30 mA; scanning speed 0.02°/sec). The instrument was operated in 2θ scale with an angular range of 2–40° at a scan rate of 0.0499°/s.

2.4.4. Scanning Electron microscopy (SEM)

The shape and surface morphology was observed using SEM (JEOL-JSM-6380LVERDA, USA). The study was conducted with a working distance of 7 mm. The frequency of Electron Gun was kept at 10 kV. The samples were placed on the aluminium stubs previously stacked with double-sided sticky carbon tape separately and placed each stub in their proper position marked on the stage of the instrument. The analysis was done under vacuum and photographs were captured at various magnifications to observe surface morphology, shape and size of each sample.

2.5. Physicochemical properties

2.5.1. Apparent solubility study

Apparent solubility of NIM, physical mixtures, control sample and synthesised NIM-NIC crystals were determined in distilled water, 0.1 N HCl (adjusted to pH 1.2), gastric fluid at fasting (Fa-SGF) without enzyme and phosphate buffer pH 8.4. An excess amount of samples were added separately into the screw-capped bottle containing 5 ml of solvent. The samples were placed in a cryostatic constant temperature reciprocating shaker bath (Tempo Instruments and Equipment Pvt. Ltd., Mumbai, India) at the temperature 25 ± 1 °C with constant shaking at 120 RPM for 48 h to allow saturation. The solutions were centrifuged (Remi Laboratory Instrument, Mumbai, India) and the supernatant was filtered through Whatman filter paper no. 41 [30]. The filtrate was analysed spectrophotometrically (UV-1800, Shimadzu, Japan) at 300 nm.

2.5.2. % Yield and drug loading efficiency

The practical yield of samples was calculated using Eq. (1). Drug loading efficiency was found by dissolving prepared samples equivalent to 10 mg of NIM in 100 ml methanol and mixed well. The resulting solution was filtered through Whatman filter paper No. 41 and filtrate was analyzed spectrophotometrically at 300 nm (Eq. (2)).

$$\%\text{Yield} = \frac{\text{Total weight of prepared sample}}{\text{Total weight of drug and coformer}} \times 100 \quad (1)$$

$$\%\text{Drug loading efficiency} = \frac{\text{Drugen trapped as crystals}}{\text{Theoritical drug content}} \times 100 \quad (2)$$

2.5.3. Moisture sorption study

The hygroscopic behaviour of powders was determined by storing spray dried powders in sealed desiccators containing saturated salt solutions, which maintained a specific relative humidity depending on the type of salt. The salts used and the corresponding relative humidities were magnesium chloride (33.0% RH), magnesium nitrate (52.8% RH), ammonium nitrate (65.0% RH), sodium chloride (75.3% RH), and potassium chloride (84.3% RH) [31]. The moisture uptake of pure NIM, control sample and cocrystallized sample was evaluated after one month via loss-on-drying.

2.5.4. Micromeritic and surface topography study

The optical microscope with CCD (charge-coupled device camera) was used to observe as well as to take photomicrographs of the pure NIM, control sample and cocrystallized samples and photomicrographs of all were used to compare morphological changes under 10X magnification. Size analysis was performed using optical microscopy method (Leica, Germany). The size and size distribution of particles were counted using eyepiece micrometre, which was previously calibrated using stage micrometre. Particle size was determined by taking the longest dimension of the particle for a minimum of 100 particles. Mean aspect ratio (AR), defined as the ratio of the length (longest dimension from edge to edge of a particle arranged parallel to the ocular scale) to the width (the longest dimension of the particle measured at a right angle of the length) of the particle, was calculated. The size of 100 randomly selected particles from the prepared batch was measured and appropriate geometric mean diameter (dg) was calculated [32].

2.5.5. Flowability study

The flow properties of pure NIM and cocrystallized samples were determined in terms of Angle of repose using the fixed funnel method. Percentage compressibility (Carr's Index) and Hausner's ratio were calculated by tapping a fixed amount of sample using tapped density tester (ETD-1020, Electrolab, Mumbai, India) (USP) [33].

2.6. Packability, compactibility and compressibility properties

2.6.1. Kawakita constants

The packability of the samples was investigated by tapping them into a 100 ml graduated cylinder (at least 60% filled) using a Tap density tester USP (Elactrolab, ETD-1020, Mumbai, India). The powder was gently poured into a graduated cylinder and the weight of the powder was measured. The bulk density (minimum density) was calculated from the powder weight divided by volume. Then the cylinder was tapped and the reduced volume was recorded after every 100 taps till the volume remained constant even after the continuous tapping [34].

For Kawakita equation,

$$\frac{n}{c} = \frac{n}{a} + \frac{1}{ab} \tag{3}$$

where a and b are the constants.

a = Value of initial porosity of the powder bed, degree of volume reduction for the bed of particles at infinite applied pressure.
1/b = Pressure needed to compress the powder to one half of the total volume.
The values of 'a' and 'b' were calculated from the slope and intercept of the linear plot of n/(c) Vs n, respectively.
n = tap number.
C = volume reduction.
'C' can be calculated according to the following equation.

$$C = \frac{V_0 - V_n}{V_0} \tag{4}$$

where, V_0 and V_n are the powder bed volumes at initial and nth tapped state, respectively.

2.6.2. Kuno's constant

The data obtained during kawakita analysis was also analysed by Kuno's equation [35].

$$\ln(qt - qn) = -Kn + \ln(qt - q0) \tag{5}$$

where,

q0, qn and qt are the initial density, density at 'nth' taps and density at infinite taps, respectively.
Kn is the Kuno's constant represents the rate of the packing process.
a, b and K are the constants representing packability of powder under mechanical force.

2.6.3. Heckel plot study

Precisely weighed quantity of cocrystallized samples (240 ± 5 mg), control batch and pure NIM (250 ± 5 mg, each) were compressed separately using 8-mm flat-faced punch in KBr press (Techno-search Instruments, Thane, India) at a constant compression at different force ranging from 1 to 9 tons (9.8×103–88.26×103 Newton) by keeping 2 min dwell time. The punch and die were lubricated using 1% w/v dispersion of magnesium stearate in acetone. The compression behaviour of prepared samples was expressed as parameters of Heckel equation. A plot of ln [1/(1 − D)] versus P was drawn and values of K, A and σ0 were gained [36].

$$\ln[1/(1 - D)] = KP + A \tag{6}$$

where,

D is the relative density of compacts; P is the applied force; K is the slope of Heckel plot (K = 1/Py) where Py is the mean yield pressure. The constant 'A' expresses the densification at low pressure; σ0 is yield strength where, σ0 = 1/3 K. Here, True density was considered as the density (mass by volume) of compacts when the highest force was applied on the powder (here, 9 ton). The relative density of compact was calculated as the ratio of density at pressure P and true density.

2.6.4. Elastic recovery study

The compacts of pure drug and cocrystallized samples prepared for Heckel analysis were studied for Elastic recovery test. The thickness of the compacts was measured immediately after ejection (Hc) and after the 24 h relaxation period (He). Elastic recovery was calculated using the equation [36].

$$\%\ ER = [(He - Hc)/Hc] \times 100 \tag{7}$$

2.6.5. Tensile strength measurement

The Prepared compacts for Heckel parameter study were subjected to the force (P) required for breaking it after 24 h relaxation with the help of Monsanto hardness tester. The tensile strength (T, Kg) of the compacts was calculated using the following equation [37].

$$T = (0.0624 \times P)/(D \times L) \tag{8}$$

where, D = the diameter of the compacts.
L = thickness (cm) of the compacts.
P = force (Kg/cm2) required to break compacts.

2.7. Formulation and evaluation of directly compressible tablets

Tablets containing an equivalent amount of NIM were prepared by direct compression using different formulation excipients of the directly compressible type as described in Table 1. The blend was introduced manually into the die and compressed in a tablet machine. The compaction surfaces were lubricated with 2% w/w magnesium stearate in acetone before compaction. The blend was compressed on an eight-station rotary tablet machine (Karnawati engineering Ltd., India) to obtain tablets of required hardness and thickness. The tablets were studied in three replicates. The compacts were ejected and stored in a screw-capped bottle for 24 h before using, to allow for possible hardening and elastic recovery. The compacts were also taken for in-process and finished product evaluation tests. The same technique was applied for the formulation of tablets of pure drug and control batch crystals. The thickness of the tablets was obtained by digital Vernier callipers. Weight variation test was carried out by weighing 20 tablets individually and then calculating the average weight. Hardness and friability of tablets were measured with help of Digital hardness tester (Electrolab Pvt. Ltd., Mumbai, India) and Roche friabilator (EF-2, Electrolab Pvt. Ltd., Mumbai, India), respectively. The disintegration time of tablets was measured using disintegration test apparatus (ED2, Electrolab Pvt. Ltd., Mumbai, India). The test was carried out by evaluating six tablets at 37 ± 1 °C in 900 ml of distilled water in accordance with the United States Pharmacopoeia 29.

2.8. In-vitro dissolution study

Cumulative percentage drug release study of pure NIM, control samples, physical mixture and cocrystallized samples, as well as their dosage forms, were carried out in 900 ml of 0.1 N HCl (pH 1.2), distilled water, pH 8.4 alkaline borate buffer solution and 300 ml of Fa-SGF at 50 RPM maintained at 37 ± 0.5°C in a dissolution apparatus USP type-II (USP Electrolab – TDT − 060P, Mumbai, India) [38]. 5 ml samples of dissolution media were withdrawn at selected time intervals and filtered through Whatman filter paper no. 41. The concentration of drug was determined by spectrophotometrically (UV-1800, Shimadzu, Japan) at 300 nm by diluting with respective buffer solution using the same media as blank. The dissolution data were analysed statistically by model-independent parameters [39,40] calculated at different time intervals, such as dissolution percentage (DP), dissolution efficiency (% DE), similarity factor f_2 and MDT *in vitro*.

2.9. Stability study

Physical and chemical stability of pure drug and cocrystallized samples (powder and tablet formulation) was assessed by storing them at the accelerated condition as per ICH guideline. The accelerated condition was 40 °C/75% RH for six months (Remi, India) and samples were placed in glass vial covered with aluminium foil. At the end of the study, the sample was evaluated by comparisons of FT-IR, DSC spectra and *in vitro* dissolution study.

3. Result and discussion

3.1. Construction of thermal-composition phase diagram

Out of several methods, thermal analysis can be one of the best methods to determine whether any interaction happens between drug and coformer or not [41]. Based on the thermal phase diagrams, one can predict a type of interaction between two components [15]. Preliminarily fusion experiment was carried out for the screening purpose using a DSC instrument. Fig. 3 shows the DSC overlay of the NIM-NIC binary mixtures at various compositions. The study was conducted at a lower heating rate (here 5 °C/min) as at higher heating rate few events of phase changes might not appear [17]. Out of all other molar ratios, 4:6 and 3:7 ratios showed endothermic peaks at very near positions. All other mixtures of NIM and NIC showed two distinct endothermic events. Hence, a molar ratio of 3.33:6.66 was selected for further thermal analysis. A single endothermic event was observed at 112.43 °C (ΔH_f = 100.88 J/g). Moreover, this melting endotherm was lower than the melting points of pure NIM (150.57 °C) and NIC (131.62 °C). This event suggested the formation of the new solid phase. Fig. 4 illustrated that the first peak consistently appeared near 110 °C, indicating the eutectic reaction. This temperature is also known as the temperature of solidus (TSolidus/°C) on a phase diagram. TLiquidus/°C was the second peak generally wider, indicating that complete melting took place over a temperature range. The resulting phase diagram depicted a "V"-type pattern which in term confirmed the eutectic formation instead of a formation of cocrystal [13].

3.2. Solid state characterization

3.2.1. DSC study

The screening of the various molar compositions confirmed a eutectic formation at 1:2 M ratio of NIM and NIC, respectively. The DSC tracing of cocrystallized samples showed a single endothermic transition with a peak of 112.43 °C (ΔH_f = 100.88 J/g). The DSC peaks of pure components, physical mixture and the prepared samples by various methods are shown in Fig. 5. The physical mixture of NIM and NIC (1:2) demonstrates an endothermic peak corresponds to the melting point of individual components.

3.2.2. FT-IR analysis

FT-IR spectra of NIM, NIC, physical mixture, control batch and eutectic are given in Fig. 6. The study of IR spectra of NIM demonstrated the characteristic absorption bands at 3282 cm^{-1} (N—H stretching vibration), 1588 cm^{-1} (aromatic rings), 1154 cm^{-1} &

Table 1
Manufacturing formulas for the preparation of directly compressible tablets.

Sr. No.	Ingredient	Amount per tablet (mg)		
		Pure drug	Control batch	Thermally fused Eutectic sample
1.	Nimesulide	100	100	196.1 mg (equivalent to 100 mg of the drug)
2.	MCC Avicel -PH 102	21	21	21
3.	Aerosil	1	1	1
4.	Mannitol	105	105	9.9
5.	Talc	5	5	5
6.	Magnesium stearate	5	5	5
7.	Crospovidone	12	12	12
	Total weight of the tablet	250	250	250

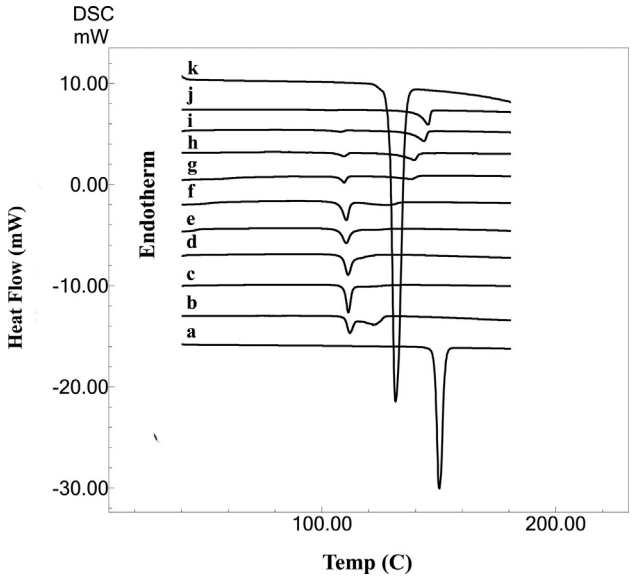

Fig. 3. Overlay of DSC endotherms for screening the eutectic composition of different molar ratios of Nimesulide (NIM): Nicotinamide (NIC) were (a) Pure NIM; (b) 1:9; (c) 2:8; (d) 3:7; (e) 4:6; (f) 5:5; (g) 6:4; (h) 7:3; (i) 8:2; (j) 9:1; (k) Pure NIC.

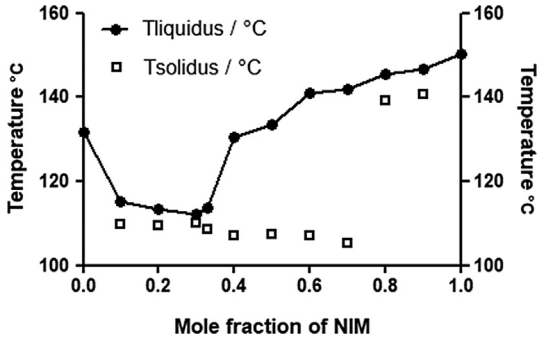

Fig. 4. Thermal-composition phase diagram of Nimesulide and Nicotinamide.

1347 cm^{-1} (SO2 anti-symmetric stretch), 1521 cm^{-1} (aromatic nitro group), respectively. The spectrum of NIM appeared at 3366.3 cm^{-1} (—NH_2 stretching vibration of primary amine), 1682 cm^{-1} (C═0 stretching vibration of primary amide), 1619 cm^{-1} (—NH_2 banding vibration), 1394.5 cm^{-1} (C—N stretching vibration of aromatic amine). The Spectrum of eutectic exhibited all the characteristic peaks of NIM as well as NIC. Furthermore, broadening of the region between 3400 cm and 1–2700 cm^{-1} was due to the formation of the weak hydrogen bond as well as lower stretching frequencies of primary —NH_2 group. It indicated no strong interaction between NIM and NIC in absence of any new or additional peak [13].

3.2.3. PXRD analysis

The new and distinct diffractogram is the evidence of the generation of a new crystal phase. In the case of NIM (Fig. 7(A)) revealed high-intensity reflections with characteristic sharp peaks at 12.01, 19.30, 21.64, 23.10 and 23.98 (2θ). As shown in Fig. 7(B), the PXRD spectra of the cocrystallized sample showed closely similar PXRD patterns with lower intensity than the physical mixture which illustrated that NIC was formed eutectic with NIM. Reduction in peak intensities in PXRD spectra was an indication of a reduction in its crystallinity [42].

3.2.4. SEM analysis

The SEM study was performed to identify and compare the morphological characteristic of NIM, NIC as against the eutectics which have manifestly distinct morphology provide a useful tool in identifying the eutectics as separate entities from their parent drug. A perusal from Fig. 8(A), pure NIM appeared as the smaller and irregular shaped crystalline particles. A tendency of formation of agglomerate was probably due to charge distribution on its surface [43]. It might have retarded its Flowability. Fig. 8(B) showed that control batch crystals were larger in its particle size, which might improve the flowability compared to the pure drug [44]. SEM images of the eutectic mixture (Fig. 8(C)) depicted a change in its appearance. The shape of the crystals was almost the same in all directions with little larger in size. It was an indication of the improvement of its flowability [34].

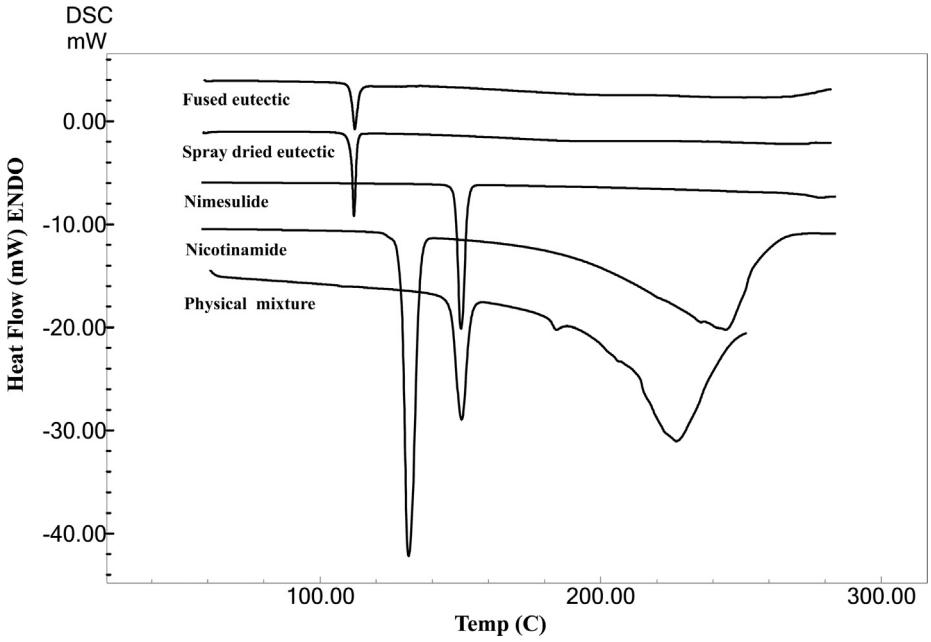

Fig. 5. DSC thermograms of (A) Fused Eutectic mixture; (B) Spray dried Eutectic mixture; (C) Pure drug Nimesulide; (D) Nicotinamide and (E) Physical mixture of Nimesulide and Nicotinamide.

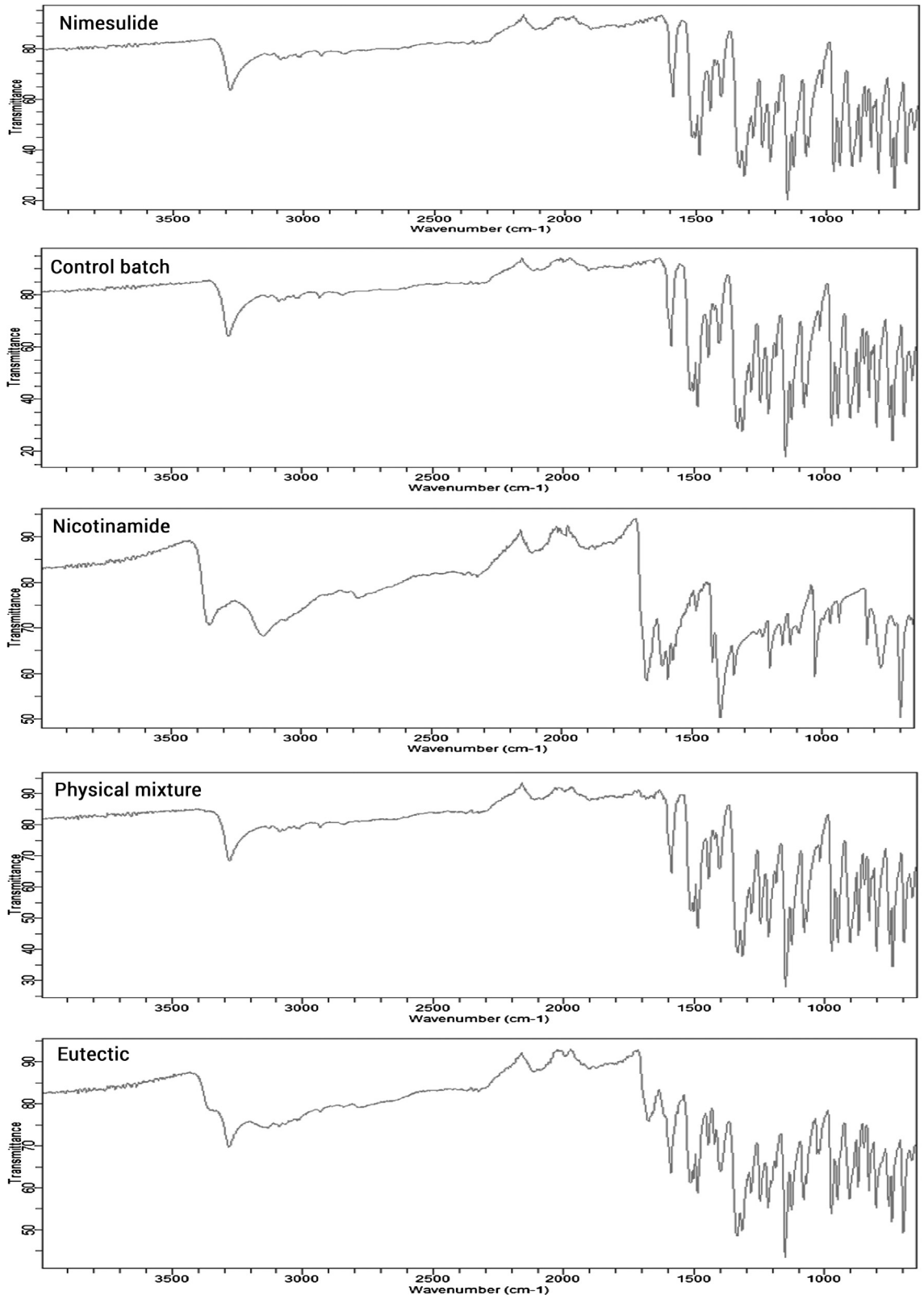

Fig. 6. FT-IR Spectra of (A) Nimesulide; (B) Control Batch; (C) Nicotinamide; (D) Physical mixture of Nimesulide and Nicotinamide and (E) Fused Eutectic mixture.

3.3. Physicochemical properties

3.3.1. Apparent solubility study

Fig. 9 represents a graphical apparent solubility of the pure drug, control batch, physical mixture and prepared eutectic in different solvents (distilled water, 0.1 N HCl, Fa-SGF without enzyme and phosphate buffer pH 8.4). The solubility of NIM in distilled water, 0.1 N HCl, pH 8.4 buffer, Fa-SGF solutions was found to be 0.040 mg/ml, 0.021 mg/ml, 0.053 mg/ml, 0.019 mg/ml, respectively. The results revealed that the drug was poorly soluble in

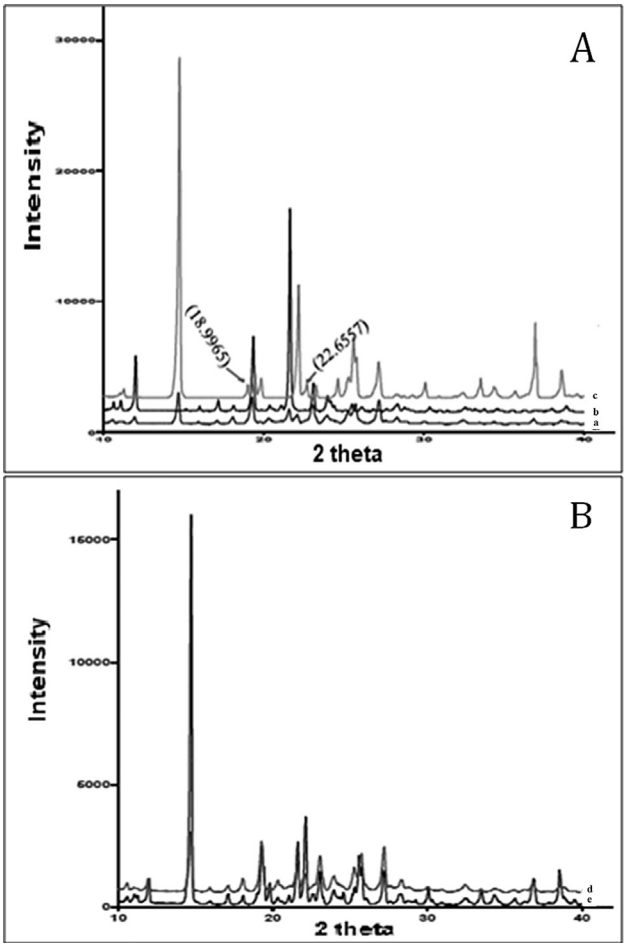

Fig. 7. (A) Comparison of Powder XRD patterns of (a) Nicotinamide; (b) Nimesulide; (c) eutectic mixture and (B) Comparison of PXRD patterns of (d) eutectic mixture; (e) Physical mixture.

acidic media due to the weakly acidic nature of the drug itself [45]. The same kind of behaviour was also observed in the control batch. It was interesting to note that the solubility of prepared eutectics exhibited higher than their physical mixtures vis-a-vis parent drug in all three media. The results were in pH 8.4 buffer (0.851 mg/ml), distilled water (0.571 mg/ml) and 0.1 N HCl (0.310 mg/ml) solutions whereas low in Fa-SGF (0.267 mg/ml) solution compared to both pure drug as well as control batch. At the same time, the solubility of NIM from the physical mixture was found to be 0.235, 0.045, 0.351 and 0.032 respectively. The solubility rise in case of physical mixture and eutectic sample was almost 5.9 and 14 times in distilled water compared to pure drug. The rise in solubility might be due to the presence of coformer, which was very much water soluble as well as a reduction in crystallinity in the eutectic sample compared to the pure drug [46].

3.3.2. % Yield and drug loading efficiency

% yield and drug loading efficiency of the prepared eutectic sample showed 71 ± 3% and 92.27 ± 4.73%, respectively which showed satisfactory results.

3.3.3. Moisture sorption study

Fig. 10 shows that the eutectic sample could not absorb much amount of moisture. It indicated a non-hygroscopic behaviour of the eutectic sample. Though, compared to the pure drug, the eutectic sample was little hygroscopic in nature. This behaviour was probably due to an interaction of the coformer molecule with the drug in eutectic formation. The relative resistance of the samples to moisture sorption followed the order: NIM > Eutectic sample > NIC. As expected, NIC is the most hygroscopic, displaying the potential affinity for water vapour. Co-crystallization with the hydrophobic former i.e. NIM substantially reduced the moisture sorption tendency of NIC by two-fold.

3.3.4. Micromeritic and surface topography study

The geometric mean diameter of the eutectic sample, control batch and the pure drug were 74.3, 64 and 59.5 μm, respectively. The aspect ratio (AR) in case of the pure drug, control batch and the eutectic sample was 3.5 ± 0.02, 1.7 ± 0.10 and 1.8 ± 0.08, respectively. The results of higher particle size, as well as reduced aspect ratio, suggested that the resulting eutectic sample was much improved in its physical properties [47].

3.3.5. Flowability study

As per the data are shown in Table 2, it was found that the flow property of pure drug was very poor. It might be due to very small particles with a strong affinity to aggregate due to the electrostatic charge generated on its surface with an irregular shape. A remarkable improvement in flow property of control batch and the eutectic sample was observed compared to pure drug. It might be because of the increase in the particle size and reduction in AR imparted sphericity to the particles [48].

3.4. Packability, compactibility and compressibility studies

3.4.1. Kawakita and Kuno's constant

Table 3 was illustrated that the lower values of 'a' and '1/b' of prepared eutectic with pure NIM and control batch in Kawakita equation were the sign of improvement in packability of eutectic compared to the pure drug. Moreover, higher K value (Kuno's constant) demonstrated better packing behaviour of treated eutectic [10].

3.4.2. Heckel plot analysis

The Heckel plot equation describes the force and displacement data to a linear relationship for the materials undergoing compaction. Densification behaviour of prepared eutectic was studied by Heckel plot analysis [49]. The true density of eutectic (2.78 g/cc), pure NIM (2.20 g/cc) and control (2.2 g/cc) suggested that the eutectic showed improvement in its packability and compaction properties compared to pure drug. Table 3 and Fig. 11 shows parameters of Heckel plot in which lower "A" value compared to pure drug indicated that low compression pressure was required to obtain the closest packing, fracturing its texture and densifying the fractured particles in case of the eutectic. Moreover, lower value of yield strength (σ0) and yield pressure (Py) compare to the pure drug was suggested that eutectic exhibited low resistance to applied pressure due to its plastic nature and fragmentation, which imparted good densification and easy compaction to the material. Thus, Heckel plot data confirming better plastic deformation of eutectic under applied compression pressure. The compressibility of the material is its ability to be reduced in volume as a result of applied pressure and is represented by a plot of % porosity against compression pressure [50]. Fig. 12 has depicted that a reduction in % porosity was observed from highest to lowest in the trend of eutectic > Control > Nimesulide.

3.4.3. Elastic recovery and tensile strength measurement

% Elastic recovery of prepared pellets was described in Table 3. It shows that the elastic recovery of the pure drug was higher compare to prepared eutectic indicating the behaviour of lamination. At the same time, elastic recovery of eutectic pellets was very small suggesting strong interparticulate bonding. Tabletability is the

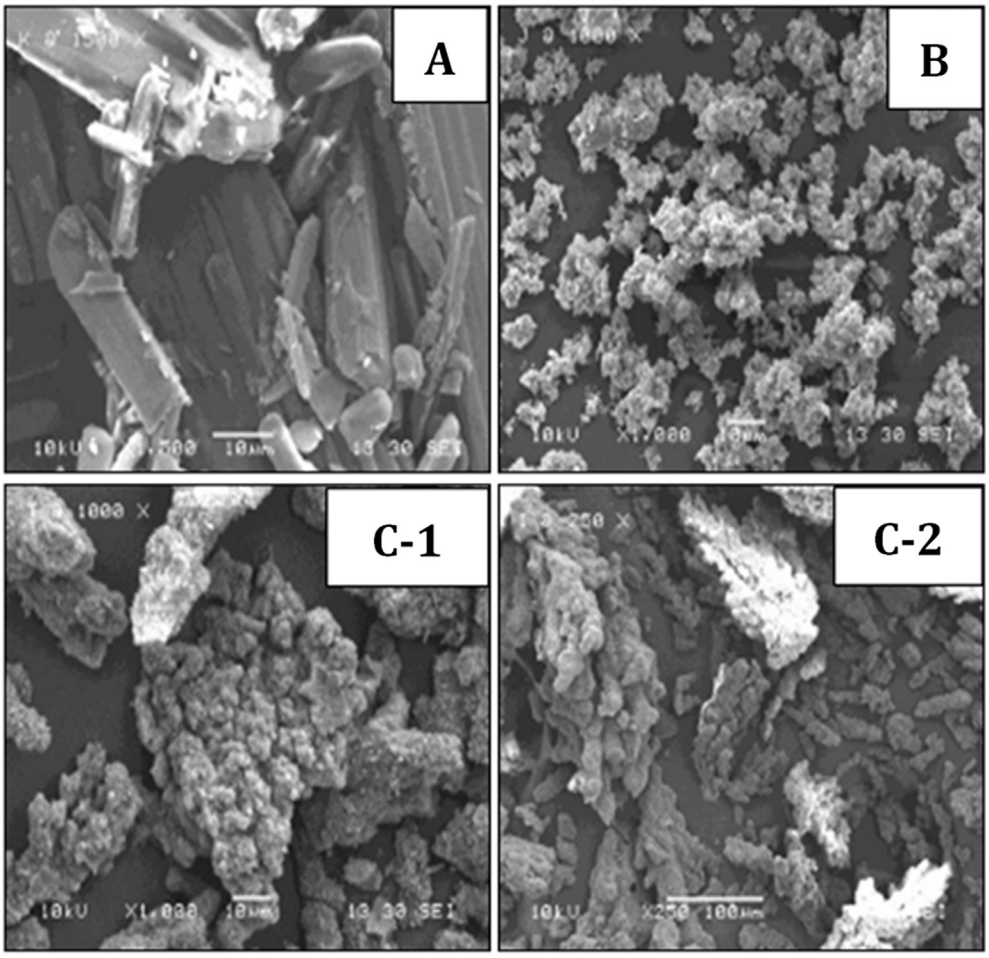

Fig. 8. SEM images of (A) pure drug; (B) control batch; (C-1) and (C-2) prepared eutectic.

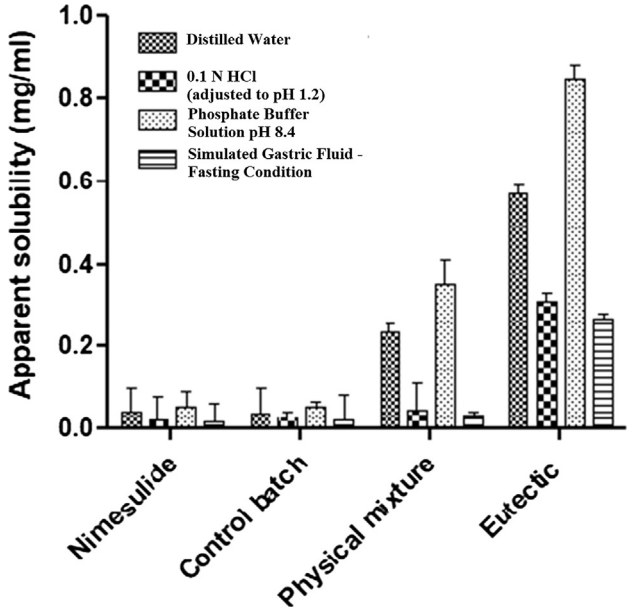

Fig. 9. Saturation solubility of Nimesulide (NIM), control batch, physical mixture and eutectic mixture in Distilled water, 0.1 N HCl (Adjusted to pH 1.2), Phosphate buffer pH 8.4 and Simulated gastric fluid at fasting condition.

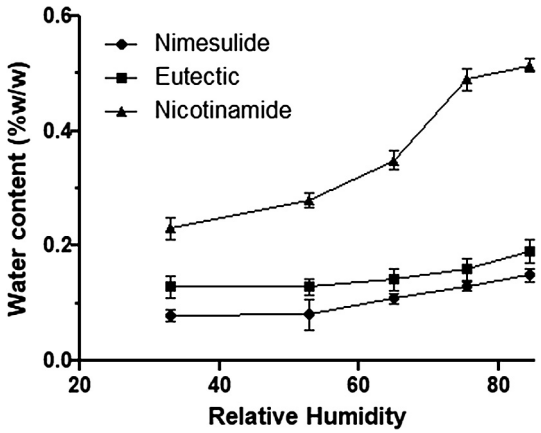

Fig. 10. Moisture sorption study of Nimesulide (NIM); Nicotinamide (NIC) and eutectic mixture in various humidity conditions.

capacity of the powder material to be transformed into a tablet of specified strength under applied compaction pressure [50]. The tensile strength of pellets (8 mm diameter) of all samples was increased with applied pressure (Table 3). However, eutectic showed higher tensile strength over parent drug at all compression pressure (Fig. 13). Thus, eutectic confirmed increased tabletability as compared to NIM. At 1 tone and 9 tone pressure, tensile strength

Table 2
Micromeritic parameters of the prepared eutectic.

Sr. no.	Parameter*	Pure drug	Control batch	Eutectic sample
1	Angle of repose	64.73 ± 0.562	33.35 ± 0.320	32.28 ± 0.213
2	%Carr's compressibility index	30.01 ± 0.156	15.31 ± 0.582	15.36 ± 0.158
3	Hausner's ratio	1.488 ± 0.018	1.286 ± 0.148	1.181 ± 0.231

* Indicates data shown as mean ± SD, (n = 3).

Table 3
Comparison of packability, compatibility and compressibility parameters of pure drug, control batch and eutectic sample.

Parameters	Pure drug	Control batch	Eutectic sample
a = 1/m	0.404	0.299	0.210
1/b = c/m	53.30	42.92	37.81
Kuno's constant, K	0.0071	0.0084	0.0154
Heckle plot constants, K	0.159	0.2386	0.3677
A	0.6154	0.5146	0.268
Mean yield Pressure, N/m^2 Py = 1/K	6.28	4.19	2.71
Yield strength S = 1/3K	2.09	1.39	0.91
% Elastic recovery*	12.4 ± 0.837	12.1 ± 0.641	2.2 ± 0.486
Tensile strength*	5.307 ± 0.512	13.564 ± 0.897	22.558 ± 0.710

* Indicates data shown as mean ± SD, (n = 3).

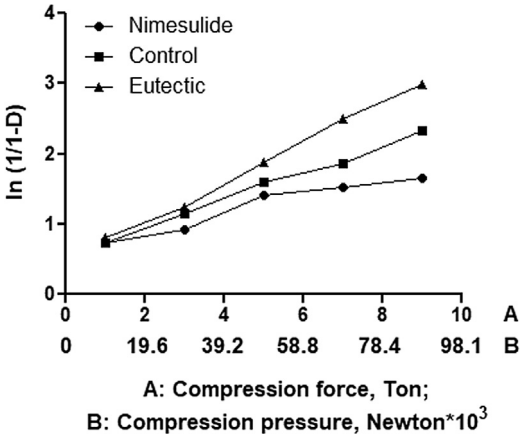

Fig. 11. Heckel plot of Nimesulide (NIM); Control batch and Prepared eutectic.

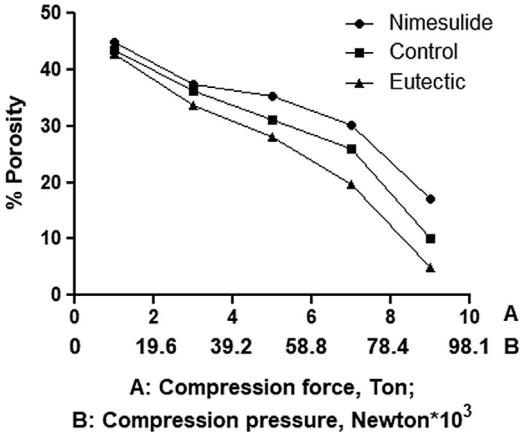

Fig. 12. Compressibility of Nimesulide (NIM); Control batch and Prepared eutectic.

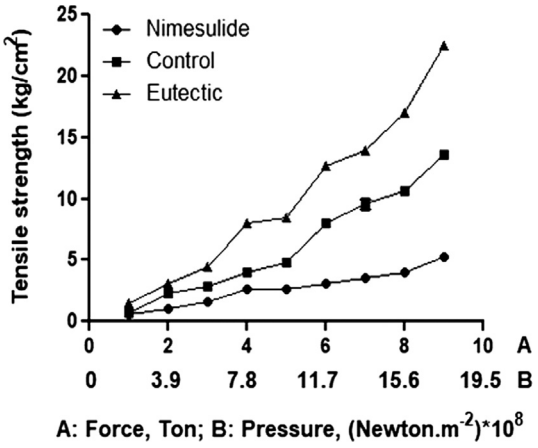

Fig. 13. Pressure – Tensile strength relation.

of eutectic and NIM was found 1.516 kg/cm^2, 0.589 kg/cm^2 and 22.558 kg/cm^2, 5.307 kg/cm^2, respectively.

3.5. Evaluation of directly compression tablets

Evaluation parameters of directly compressible tablets of pure drug, control batch and eutectic sample were performed (Table 4). All parameters were found in good agreement with the acceptance criteria [51]. The results of Table 4 shows that the physicomechanical parameters of tablets prepared from the eutectic mixture were improved compared to tablets prepared from parent drug and control batch.

3.6. In-vitro dissolution profile

As shown in Fig. 9, the eutectic samples illustrated improved solubility in distilled water compared to pure drug. The solubility results were also accompanied by its kinetic aspect and represented by the dissolution rate. Comparison of dissolution profiles (Fig. 14) of powder formulations revealed that prepared eutectic showed higher drug release (43.49%) compared to control (25.50%), pure drug (24.30%), respectively within one hour. The same kind of behaviour was also observed in the case of tablets prepared from all the samples (Fig. 15). The dissolution efficacy ($\%DE_{15\ min}$) of eutectic samples (powder as well as the tablet) were found to be improved by 4.7 and 4.9 folds, respectively compared to the pure drug (Table 4). Also, 2.9 folds improvement in $\%\ DP_{15\ min}$ of the eutectic sample (both powder and tablet) suggested its fast dissolving capability compared to the pure drug (Table 4). This enhancement of dissolution might be due to local solubilisation effects produced by nicotinamide in addition to modulate thermodynamic behaviours such as crystal packing, molecular mobility and intermolecular interaction [14]. As the drug has very poor solubility in acidic media and gastric fluid, after achieving certain concentration the dissolution media becomes almost saturated and dissolution of drug ceases. At the same time, the pure drug, as well as eutectic mixture, showed remarkable

Table 4
Evaluation and dissolution parameters of directly compressed tablets and prepared samples.

Parameters		Pure drug	Control batch	Eutectic sample
Weight variation (mg) ± SD*		251.2 ± 2.43	252.4 ± 3.12	250.5 ± 2.81
Thickness (mm) ± SD*		3.0 ± 0.21	3.2 ± 0.24	3.2 ± 0.20
Hardness (kg/cm^2) ± SD*		4.8 ± 0.31	5.2 ± 0.25	6.4 ± 0.3
Friability (% loss) ± SD*		0.26 ± 0.08	0.18 ± 0.07	0.17 ± 0.05
D.T.(sec) ± SD*		172 ± 12	179 ± 9.5	196 ± 5.8
% $DE_{15\ min}$	Powder	7.25	8.70	34.15
	Tablet	2.1	4.40	10.4
% $DP_{15\ min}$	Powder	10.04	15.33	29.13
	Tablet	8.84	15.30	25.65
f_2 Value	Powder	–	65.30	34.80
	Tablet	–	67.20	41.70
MDT, min	Powder	40.80	25.14	24.40
	Tablet	43.70	25.80	26.70

* Indicates data shown as mean ± SD, (n = 3).

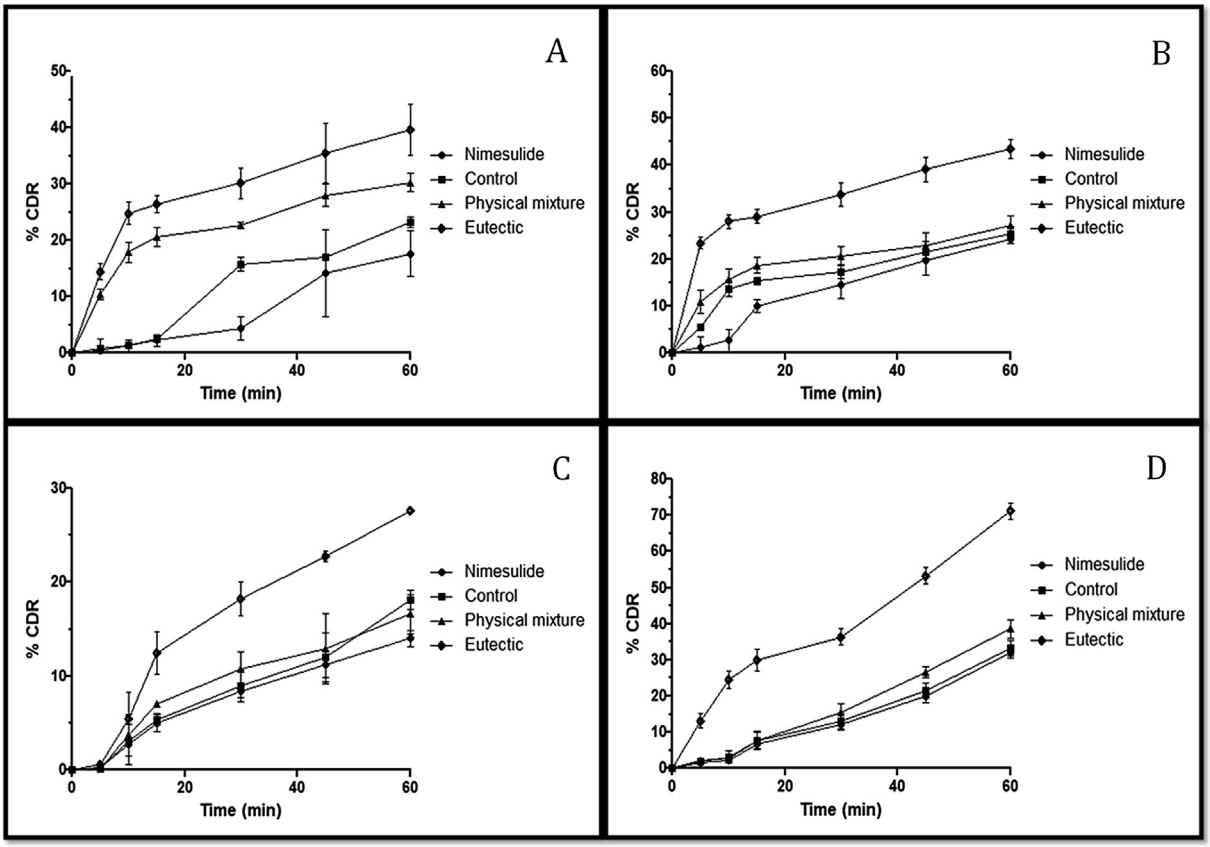

Fig. 14. *In-vitro* dissolution profile of powder formulation in (A) 0.1 N HCl (Adjusted to pH 1.2); (B) Fa-SGF; (C) Distilled Water and (D) Phosphate Buffer pH 8.4.

dissolution in alkaline borate buffer pH 8.4, because of the drug itself weakly acidic in nature [52].

3.7. Stability study

The dissolution profiles of eutectic samples were investigated to be similar before and after study. The statistical data were also proved similarity between two dissolution profiles which were found f_2 = 68.75 for powder and f_2 = 72.96 for tablet formulation before and after study. Moreover, FTIR spectra and DSC thermograms (Data not shown here) of eutectic samples also illustrated no change in their spectra and thermograms compared with the initial samples. These results suggested that prepared eutectic formulation was stable and retained its stability under the extreme condition of storage.

4. Conclusion

In the present work, NIM was selected as a model drug and was fused with NIC in various molar ratios. The drug and conformer formed eutectic with the molar ratio of 1:2. Finally, a large scale batch was prepared by spray drying by taking the above ratio. The resulted product was much improved in its physicochemical and mechanical properties compared to pure drug. Based on the FT-IR data, there might be a possibility of formation of hydrogen bond for this multi-component interaction. The resulted crystals

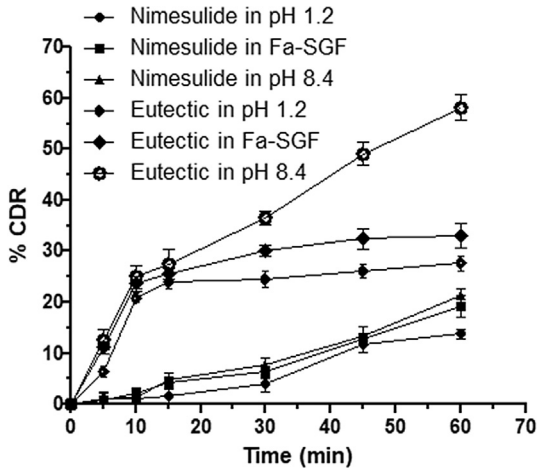

Fig. 15. *In vitro* dissolution profile of tablet formulations of the pure drug Nimesulide and eutectic mixture in 0.1 N HCl (Adjusted to pH 1.2); Fa-SGF and Phosphate buffer pH 8.4.

were near to the same shape from all the directions which facilitated to the improvement in the flow and compressibility. Accelerated stability study of prepared eutectic and its formulation indicated its stable nature. The comprehensive study envisaged that thermal technique in the development of multi-component adducts can be very much useful. Furthermore, solid-state engineering can simultaneously improve the overall functionality of the API and can be used commercially for the manufacturing of directly compressible dosage forms.

Declaration of interest

Authors are not having any declaration of interest.

Acknowledgement

The author is very much grateful to Prof. (Dr.) Arvind Bansal, Head, Department of Pharmaceutics, NIPER-Mohali and Prof. (Dr.) Changquan Calvin Sun, Professor, Department of Pharmaceutics, University of Minnesota, the USA for their continuous guidance and support throughout the study. The author also acknowledges Internal Quality Assurance Cell, Saurashtra University, Rajkot, Gujarat (I) for their financial assistance in carrying out the study.

References

[1] A.N. Lukyanov, V.P. Torchilin, Micelles from lipid derivatives of water-soluble polymers as delivery systems for poorly soluble drugs, Adv. Drug. Deliv. Rev. 56 (9) (2004) 1273–1289.
[2] S. Mallick, S. Pattnaik, K. Swain, P.K. De, A. Saha, P. Mazumdar, G. Ghoshal, Physicochemical characterization of interaction of ibuprofen by solid-state milling with aluminum hydroxide, Drug Dev. Ind. Pharm. 34 (7) (2008) 726–734.
[3] D. Bhikshapathi, P. Madhukar, B.D. Kumar, G.A. Kumar, Formulation and characterization of pioglitazone HClself-emulsifying drug delivery system, Der. Pharmacia. Lettre 5 (2) (2013) 292–305.
[4] E. Reverchon, P.G. Della, R. Taddeo, P. Pallado, A. Stassi, Solubility and micronization of griseofulvin in supercritical CHF3, Ind. Eng. Chem. Res. 34 (11) (1995) 4087–4091.
[5] G. Becket, L.J. Schep, M.Y. Tan, Improvement of the *in vitro* dissolution of praziquantel by complexation with α-, β-and γ-cyclodextrins, Int. J. Pharm. 179 (1) (1999) 65–71.
[6] K. Kawakami, N. Oda, K. Miyoshi, T. Funaki, Y. Ida, Solubilization behavior of a poorly soluble drug under combined use of surfactants and cosolvents, Eur. J. Pharm. Sci. 28 (1–2) (2006) 7–14.
[7] K. Westesen, H. Bunjes, M.H.J. Koch, Physicochemical characterization of lipid nanoparticles and evaluation of their drug loading capacity and sustained release potential, J. Control. Release 48 (2–3) (1997) 223–236.
[8] H. Chen, C. Khemtong, X. Yang, X. Chang, J. Gao, Nanonization strategies for poorly water-soluble drugs, Drug Discov. Today 16 (7–8) (2011) 354–360.
[9] M.K. Raval, P.D. Vaghela, A.N. Vachhani, N.R. Sheth, Role of excipients in the crystallization of Albendazole, Adv. Powder Technol. 26 (4) (2015) 1102–1115.
[10] M.K. Raval, J.M. Patel, R.K. Parikh, N.R. Sheth, Studies on influence of polymers and excipients on crystallization behavior of metformin HCl to improve the manufacturability, Part. Sci. Technol. 32 (5) (2014) 431–444.
[11] A.V. Trask, W.S. Motherwell, W. Jones, Physical stability enhancement of theophylline via cocrystallization, Int. J. Pharm. 320 (1) (2006) 114–123.
[12] N. Rodríguez-Hornedo, S.J. Nehm, K.F. Seefeldt, Y. Pagan-Torres, C.J. Falkiewicz, Reaction crystallization of pharmaceutical molecular complexes, Mol. Pharm. 3 (3) (2006) 362–367.
[13] S. Cherukuvada, T.N. Guru Row, Comprehending the formation of eutectics and cocrystals in terms of design and their structural interrelationships, Cryst. Growth Des. 14 (8) (2014) 4187–4198.
[14] S. Cherukuvada, A. Nangia, Eutectics as improved pharmaceutical materials: design, properties and characterization, Chem. Commun. 50 (8) (2014) 906–923.
[15] S. Cherukuvada, On the issues of resolving a low melting combination as a definite eutectic or an elusive cocrystal: A critical evaluation, J. Chem. Sci. 128 (4) (2016) 487–499.
[16] H. Yamashita, Y. Hirakura, M. Yuda, T. Teramura, K. Terada, Detection of cocrystal formation based on binary phase diagrams using thermal analysis, Pharm. Res. 30 (1) (2013) 70–80.
[17] K. Chadha, M. Karan, R. Chadha, Y. Bhalla, K. Vasisht, Is Failure of cocrystallization actually a failure? Eutectic formation in cocrystal screening of hesperetin, J. Pharm. Sci. 106 (8) (2017) 2026–2036.
[18] I. Sathisaran, S.V. Dalvi, Crystal engineering of curcumin with salicylic acid and hydroxyquinol as conformers, Cryst. Growth Des. 17 (7) (2017) 3974–3988.
[19] H. Jain, K.S. Khomane, A.K. Bansal, Implication of microstructure on the mechanical behaviour of an aspirin–paracetamol eutectic mixture, Cryst. Eng. Comm. 16 (36) (2014) 8471–8478.
[20] S.G. Khare, S.K. Jena, A.T. Sangamwar, S. Khullar, S.K. Mandal, Multicomponent pharmaceutical adducts of α-eprosartan: physicochemical properties and pharmacokinetic study, Cryst. Growth Des. 17 (4) (2017) 1589–1599.
[21] R. Thipparaboina, D. Thumuri, R. Chavan, V.G.M. Naidu, N.R. Shastri, Fast dissolving drug-drug eutectics with improved compressibility and synergistic effects, Eur. J. Pharm. Sci. 104 (2017) 82–89.
[22] A. Górniak, B. Karolewicz, E. Żurawska-Płaksej, J. Pluta, Thermal, spectroscopic, and dissolution studies of the simvastatin–acetylsalicylic acid mixtures, J. Therm. Anal. Calorim. 111 (3) (2013) 2125–2132.
[23] J. Haneef, R. Chadha, Drug-drug multicomponent solid forms: cocrystal, coamorphous and eutectic of three poorly soluble antihypertensive drugs using mechanochemical approach, AAPS PharmSciTech. 18 (6) (2017) 2279–2290.
[24] R. Chadha, M. Sharma, J. Haneef, Multicomponent solid forms of felodipine: preparation, characterisation, physicochemical and in-vivo studies, J. Pharm. Pharmacol. 69 (3) (2017) 254–264.
[25] E. Batisai, A. Ayamine, O.E. Kilinkissa, N.B. Báthori, Melting point–solubility–structure correlations in multicomponent crystals containing fumaric or adipic acid, Cryst. Eng. Comm. 16 (43) (2014) 9992–9998.
[26] S. Budavari, M.J. O'Neil, A. Smith, P.E. Heckelman, J.R. Obenchain Jr, J.A.R. Gallipeau, M.A. D'Arecea, The Merck Index, An Encyclopedia of Chemicals, Drugs, and Biologicals, 13th, White house Station, Merck & Co, NJ, 2001.
[27] V.R. Hathwar, R. Pal, T.N. Guru Row, Charge density analysis of crystals of nicotinamide with salicylic acid and oxalic acid: an insight into the salt to cocrystal continuum, Cryst. Growth Des. 10 (8) (2010) 3306–3310.
[28] G. Diarce, I. Gandarias, A. Campos-Celador, A. García-Romero, U.J. Griesser, Eutectic mixtures of sugar alcohols for thermal energy storage in the 50–90 C temperature range, Sol. Energy Mater. Sol. Cells. 134 (2015) 215–226.
[29] A. Alhalaweh, W. Kaialy, B. Graham, G. Hardyal, N. Ali, P.V. Sitaram, Theophylline cocrystals prepared by spray drying: physicochemical properties and aerosolization performance, AAPS PharmSciTech. 14 (2013) 265–276.
[30] S. Rawat, S.K. Jain, Solubility enhancement of celecoxib using β-cyclodextrin inclusion complexes, Eur. J. Pharm. Biopharm. 57 (2) (2004) 263–267.
[31] Y. Gonnissen, J.P. Remon, C. Vervaet, Development of directly compressible powders via co-spray drying, Eur. J. Pharm. Biopharm. 67 (2007) 220–226.
[32] H.G. Brittain, Particle size distribution representation of particle shape, size and distribution, Pharm. Technol. 25 (12) (2001) 38–45.
[33] F.M. Thomson, Storage and Flow of Particulate Solids, in: Handbook of Powder Science & Technology, Springer, Boston, MA, 1997, pp. 389–486.
[34] M.K. Raval, K.R. Sorathiya, N.P. Chauhan, J.P. Patel, R.K. Parikh, N.R. Sheth, Influence of polymers/excipients on development of agglomerated crystals of secnidazole by crystallo co- agglomeration technique to improve processability, Drug Dev. Ind. Pharm. 39 (3) (2013) 437–446.
[35] N. Patra, S.P. Singh, P. Hamd, M. Vimladevi, A systematic study on micromeritic properties and consolidation behavior of the terminaliya arjuna bark powder for processing into tablet dosage form, Int. J. Pharma. Excip. 6 (2007) 6–10.
[36] M. Maghsoodi, D. Hassan-Zadeh, M. Barzegar-Jalali, Improved compaction and packing properties of naproxen agglomerated crystals obtained by spherical crystallization technique, Drug Dev. Ind. Pharma. 33 (2007) 1216–1224.
[37] B.S. Barot, P.B. Parejiya, T.M. Patel, R.K. Parikh, M.C. Gohel, Development of directly compressible Metformin hydrochloride by the spray-drying technique, Acta. Pharm. 60 (2010) 165–175.
[38] K. Sandra, The use of biorelevant dissolution media to forecast the in vivo performance of a drug, AAPS J. 12 (3) (2010) 397–407.

[39] N.H. Anderson, M. Bauer, N. Boussac, R. Khan-Malek, P. Munden, M. Sardaro, An evaluation of fit factors and dissolution efficiency for the comparison of *in-vitro* dissolution profiles, J. Pharm. Biomed. Anal. 17 (4–5) (1998) 811–822.
[40] N. Schultheiss, A. Newman, Pharmaceutical co-crystals and their physicochemical properties, Cryst. Growth Des. 9 (6) (2009) 2950–2967.
[41] H. Yamashita, Y. Hirakura, M. Yuda, K. Terada, Coformer screening using thermal analysis based on binary phase diagrams, Pharm. Res. 31 (8) (2014) 1946–1957.
[42] P.P. Shah, R.C. Mashru, Development and evaluation of artemether taste masked rapid disintegrating tablets with improved dissolution using solid dispersion technique, AAPS PharmSciTech. 9 (2) (2008) 494–500.
[43] A.K. Tiwari, Modification of crystal habit and its role in dosage form performance, Drug Dev. Ind. Pharm. 27 (7) (2001) 699–709.
[44] S. Mallick, Effect of solvent and polymer additives on crystallization, Indian J. Pharm. Sci. 66 (2) (2004) 142–147.
[45] A. Bennett, G. Villa, Nimesulide: an NSAID that preferentially inhibits COX-2, and has various unique pharmacological activities, Exp. Opin. Pharmaco. 1 (2) (2000) 277–286.
[46] P.J. Marsac, S.L. Shamblin, L.S. Taylor, Theoretical and practical approaches for prediction of drug–polymer miscibility and solubility, Pharm. Res. 23 (10) (2006) 2417.
[47] S.P. Bhattacharyya, I. Bhattacharyya, N. Patro, Standarization and optimization of micromeretic properties of nimesulide for processing into a tablet dosage form by crystalo-co-agglomeration technology, Asian J. Pharm. 4 (1) (2014) 24–27.
[48] Y. Kawashima, M. Imai, H. Takeuchi, H. Yamamoto, K. Kamiya, T. Hino, Improved flowability and compactibility of spherically agglomerated crystals of ascorbic acid for direct tableting designed by spherical crystallization process, Powder Technol. 130 (2003) 283–289.
[49] S. Patel, A.M. Kaushal, A.K. Bansal, Effect of particle size and compression force on compaction behaviour and derived mathematical parameters of compressibility, Pharm. Res. 24 (1) (2007) 111–124.
[50] C.C. Sun, Decoding powder tabletability: roles of particle adhesion and plasticity, J. Adhes. Sci. Technol. 25 (4–5) (2011) 483–499.
[51] L. Dobetti, Fast-melting tablets: developments and technologies, Pharm. Technol. 25 (9) (2001) 44–50.
[52] B.N. Nalluri, K.P.R. Chowdary, K.V.R. Murthy, G. Becket, A.R. Hayman, Physicochemical characteristics and dissolution properties of nimesulide–cyclodextrin binary systems, AAPS PharmSciTech. 4 (1) (2003) 6.